2013 American Control Conference (ACC)
Washington, DC, USA, June 17-19, 2013

Inversion-Free Adaptive Control of Uncertain Systems with Shape-Memory-Alloy Actuation

Mohammad Al Janaideh and Dennis S. Bernstein

Abstract— **We apply retrospective cost adaptive control (RCAC) to a command-following problem for an uncertain shape-memory-alloy (SMA) actuator. The SMA actuator is characterized by a Wiener model consisting of linear dynamics that convert the input voltage or current to a temperature, and a hysteresis model that characterizes the relationship between the temperature and the output displacement. We use the generalized Prandtl-Ishlinskii model to characterize the input-output relationship between the temperature and the output displacement in the SMA actuator.**

I. Introduction

In many control applications, the primary source of nonlinearity is often not the plant per se, but rather the actuation, which gives rise to an input nonlinearity. For example, the input nonlinearity may represent the properties of an actuator, such as saturation to reflect magnitude restrictions on the control input, deadzone to represent actuator stiction, or a signum function to represent on-off operation. The ability to invert the nonlinearity may be precluded in practice by the fact that the nonlinearity may be neither one-to-one nor onto, and it may also be uncertain.

Beyond these basic nonlinearities lies the fact that actuators are often constructed from smart materials that have electromechanical or thermomechanical properties that make them superior to traditional devices such as rotary motors. For example, piezoelectric devices provide high force with high bandwidth and low backlash, while shape memory alloy materials provide high displacement. The challenge and opportunity in control engineering is to exploit these properties while addressing the difficulties that arise from the fact that smart materials are invariably hysteretic.

If the input nonlinearity, which may or may not be hysteretic, is uncertain, then adaptive control may be useful for learning the characteristics of the nonlinearity online and compensating for the distortion that it introduces. Adaptive inversion control of systems with uncertain input nonlinearities and linear dynamics is considered in [1, 2]. In contrast, the retrospective-cost adaptive control (RCAC) approach used in [3, 4] makes no attempt to invert the input nonlinearity. This approach is applicable to linear plants that are possibly MIMO, nonminimum phase (NMP), and unstable [5–9]. RCAC relies on knowledge of Markov parameters and, for NMP open-loop-unstable plants, estimates of the NMP zeros. This information can be obtained from either analytical modeling or system identification [10].

M. Al Janaideh is with the Department of Mechatronics Engineering, The University of Jordan, Amman 11942, Jordan. D. S. Bernstein is with the Department of Aerospace Engineering, The University of Michigan, Ann Arbor, MI 48109.

The goal of the present paper is to apply the approach used in [4, 8] to hysteretic actuators based on shape memory alloys. These materials exhibit highly hysteretic thermomechanical behavior [11–13] and thus are challenging to use in precision motion control systems. Prior applications of control for systems with SMA actuators have used inversion techniques to mitigate the effect of the hysteresis. In contrast, as in [3, 4], we apply RCAC without attempting to invert the hysteresis nonlinearity.

The contents of the paper are as follows. Section II presents a Wiener model for the SMA actuator. Section III formulates the problem. Section IV applies RCAC to a command-following problem for uncertain SMA systems. RCAC is validated for uncertain SMA systems through simulations in section V. Section VI shows the ability of the RCAC to control a flap positioning system.

II. Wiener Model Structure for the SMA Actuator

In this section we present a Wiener model for the SMA actuator. This model is described in [13]. The input to the SMA actuator is current or voltage, and the output is displacement. The SMA actuator is heated by the Joule heating process [12]. The hysteresis nonlinearity existing in the SMA is a phase transformation from the austensite phase to the martensite phase, or vice-versa. The martensite phase occurs at low temperature, where the SMA material is relatively soft, while the austensite phase occurs at high temperature, where the SMA material is relatively hard.

The relationship between the applied input voltage or current $u(t)$ and the output displacement $v(t)$ can be expressed as

$$v(t) = \mathcal{P}\big(u(t)\big), \tag{1}$$

where $\mathcal{P}$ consists of the linear actuator dynamics G_a cascaded with the hysteresis nonlinearity $\mathcal{N}$, see Figure 1. The linear system G_a represents the heating process, while the hysteresis nonlinearity represents the phase transformation between the austensite phase and martensite phase.

A. The temperature dynamics model G_a

By applying a voltage or current $u(t)$ across the SMA actuator, the temperature $u_0(t)$ is expressed as

$$\dot{u}_0(t) + \sigma u_0(t) = \eta u(t), \tag{2}$$

where σ and η are positive constants. It is important to note that the temperature $u_0(t)$ in the SMA actuator cannot

978-1-4799-0176-0/$31.00 ©2013 AACC

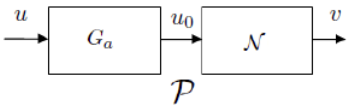

Fig. 1. Wiener model of the SMA actuator. This model consists of the linear actuator dynamics G_a cascaded with the hysteresis nonlinearity $\mathcal{N}$ appearing at the output of the linear system, where $u(t)$ is the applied input voltage or current, $u_0(t)$ is the temperature, and the output $v(t)$ is the displacement of the SMA actuator.

be measured in real time. The actuator dynamics transfer function from u to u_0 is given by

$$G_a(s) = \frac{\eta}{s+\sigma}. \tag{3}$$

B. The generalized Prandtl-Ishlinskii model

The relationship between the temperature $u_0(t)$ and the output displacement $v(t)$ can be expressed as

$$v(t) = \mathcal{N}\big(u_0(t)\big), \tag{4}$$

where $\mathcal{N}$ represents the hysteretic nonlinearity in the SMA actuator. In this paper, we use the generalized Prandtl-Ishlinskii model to represent the hysteresis nonlinearity $\mathcal{N}$. This model characterizes the hysteresis nonlinearity between the temperature u_0 and the displacement v in the SMA actuator [15–18].

Let the input signal $u_0(t)$ be continuous in $[0, T]$. The output of the generalized Prandtl-Ishlinskii model constructed as a superposition of the generalized play operators Ψ_{ρ_i} is expressed as

$$v(t) = \Phi[u_0](t) := \sum_{i=0}^{n} a_i \Psi_{\rho_i}[u_0](t), \tag{5}$$

where n is the number of generalized play operators and $a_0, \ldots, a_n$ are positive constants. In each interval of a partition

$$0 = t_0 < t_1 < \cdots < t_l = T,$$

the output of the generalized play operator Ψ_{ρ_i} for $t \in (t_{j-1}, t_j]$ can be expressed as

$$\Psi_{\rho_i}[u_0](t) = \max\big\{\gamma\big(u_0(t)\big) - \rho_i, \min\{\gamma\big(u_0(t)\big) + \rho_i, \Psi_{\rho_i}[u_0](t_{j-1})\}\big\}, \tag{6}$$

where γ is a memoryless, continuous, strictly monotonic function and ρ_i is a positive threshold.

The generalized Prandtl-Ishlinskii model (5) specializes to the Prandtl-Ishlinskii model when $\gamma(u_0) = u_0$. The generalized Prandtl-Ishlinskii model yields clockwise input-output curves that characterize hysteresis in piezoceramic and magnetostrictive actuators [15].

C. Discretization of the Wiener model $\mathcal{P}$

The discrete-time model for $\mathcal{P}$ is

$$u_0(k+1) = -\bar{\sigma} u_0(k) + \bar{\eta} u(k), \tag{7}$$

$$v(k) = \Phi\big(u_0(k)\big), \tag{8}$$

where the time step is normalized to 1 and

$$\Psi_{\rho_i}[u_0](k) = \max\big\{\gamma\big(u_0(k)\big) - \rho_i, \min\{\gamma\big(u_0(k)\big) + \rho_i, \Psi_{\rho_i}[u_0](k-1)\}\big\}. \tag{9}$$

III. Problem Formulation

Consider the Wiener command-following problem

$$x(k+1) = Ax(k) + Bv(k) + D_1 w(k), \tag{10}$$

$$y(k) = Cx(k) + D_2 w(k), \tag{11}$$

$$u_0(k+1) = -\bar{\sigma} u_0(k) + \bar{\eta} u(k), \tag{12}$$

$$v(k) = \mathcal{N}\big(u_0(k)\big), \tag{13}$$

$$z(k) = r(k) - y(k), \tag{14}$$

where $x(k) \in \mathbb{R}^n$ is the state, $r(k) \in \mathbb{R}^{l_r}$ is the command, $u(k) \in \mathbb{R}^{l_u}$ is the control, $w(k) \in \mathbb{R}^{l_w}$ is the exogenous signal for the linear plant G, $\mathcal{N}\colon \mathbb{R} \to \mathbb{R}$ is the hysteretic nonlinearity of the SMA actuator, and $z(k) \in \mathbb{R}^{l_z}$ is the command-following error. We assume that G_a is uncertain except for a limited number of Markov parameters. The hysteresis of the SMA actuator is also uncertain. A block diagram for (10)–(14) is shown in Figure 1. We apply RCAC to the SMA system in order to have the output y follow the command signal r. A block diagram for (10)-(14) is shown in Figure 2. The goal is to determine a controller that makes z small.

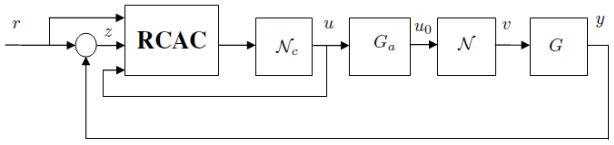

Fig. 2. Adaptive command-following problem for the SMA actuator. The discrete-time SMA model $\mathcal{P}$ is shown with the RCAC adaptive controller, auxiliary saturation nonlinearity $\mathcal{N}_c$, and the linear plant G. We assume that measurements of $z(k)$ are available for feedback; however, measurements of $v(k)$ and $u_0(k)$ are not available.

IV. Adaptive Control for Uncertain Systems with Shape-Memory-Alloy Actuation

We assume that the temperature dynamics model G_a is uncertain except for an estimate of a single nonzero Markov parameter. The input nonlinearity $\mathcal{N}$ is uncertain, and the linear system G is unknown and asymptotically stable. To account for the presence of the nonlinearity $\mathcal{N}$ of the SMA model $\mathcal{P}$, the RCAC controller in Figure 2 uses the auxiliary saturation nonlinearity $\mathcal{N}_c$ with output u_c defined by

$$\mathcal{N}_c(u_c) = \mathrm{sat}_a(u_c) = \begin{cases} -a, & \text{if} \quad u_c < -a, \\ u_c, & \text{if} \quad -a \le u_c \le a, \\ a, & \text{if} \quad u_c > a, \end{cases} \tag{15}$$

where $a > 0$ is the saturation level. For NMP plants, the saturation level a is used to tune the transient behavior. In addition, the saturation level is chosen to provide the magnitude of the control input needed to follow the command r. This level depends on the range of the input nonlinearity

$\mathcal{N}$ as well as the gain of the linear actuator dynamics G_a at frequencies in the spectra of r and w. For $i \geq 1$, define the Markov parameter

$$H_i \triangleq E_1 A^{i-1} B.$$

For example, $H_1 = E_1 B$ and $H_2 = E_1 AB$. Let ℓ be a positive integer. Then, for all $k \geq \ell$,

$$x(k) = A^\ell x(k-\ell) + \sum_{i=1}^{\ell} A^{i-1} B \mathcal{P}(\mathcal{N}_c(u_{\mathrm{c}}(k-i))), \quad (16)$$

and thus

$$z(k) = E_1 A^\ell x(k-\ell) - E_0 r(k) + \bar{H}\bar{U}(k-1), \quad (17)$$

where

$$\bar{H} \triangleq \left[\begin{array}{ccc} H_1 & \cdots & H_\ell \end{array} \right] \in \mathbb{R}^{1 \times \ell}$$

and

$$\bar{U}(k-1) \triangleq \left[\begin{array}{c} \mathcal{P}\big(\mathcal{N}_c(u_{\mathrm{c}}(k-1))\big) \\ \vdots \\ \mathcal{P}\big(\mathcal{N}_c(u_{\mathrm{c}}(k-\ell))\big) \end{array} \right].$$

Next, we rearrange the columns of $\bar{H}$ and the components of $\bar{U}(k-1)$ and partition the resulting matrix and vector so that

$$\bar{H}\bar{U}(k-1) = \mathcal{H}' U'(k-1) + \mathcal{H} U(k-1), \quad (18)$$

where $\mathcal{H}' \in \mathbb{R}^{1 \times (\ell - l_U)}$, $\mathcal{H} \in \mathbb{R}^{1 \times l_U}$, $U'(k-1) \in \mathbb{R}^{\ell - l_U}$, and $U(k-1) \in \mathbb{R}^{l_U}$. Then, we can rewrite (17) as

$$z(k) = \mathcal{S}(k) + \mathcal{H} U(k-1), \quad (19)$$

where

$$\mathcal{S}(k) \triangleq E_1 A^\ell x(k-\ell) - E_0 r(k) + \mathcal{H}' U'(k-1). \quad (20)$$

Next, for $j = 1, \ldots, s$, we rewrite (19) with a delay of k_j time steps, where $0 \leq k_1 \leq k_2 \leq \cdots \leq k_s$, in the form

$$z(k-k_j) = \mathcal{S}_j(k-k_j) + \mathcal{H}_j U_j(k-k_j-1), \quad (21)$$

where (20) becomes

$$\mathcal{S}_j(k-k_j) \triangleq E_1 A^\ell x(k-k_j-\ell) + \mathcal{H}_j' U_j'(k-k_j-1)$$

and (18) becomes

$$\bar{H}\bar{U}(k-k_j-1) = \mathcal{H}_j' U_j'(k-k_j-1) + \mathcal{H}_j U_j(k-k_j-1),$$

where $\mathcal{H}_j' \in \mathbb{R}^{1 \times (\ell - l_{U_j})}$, $\mathcal{H}_j \in \mathbb{R}^{1 \times l_{U_j}}$, $U_j'(k-k_j-1) \in \mathbb{R}^{\ell - l_{U_j}}$, and $U_j(k-k_j-1) \in \mathbb{R}^{l_{U_j}}$. Now, by stacking $z(k-k_1), \ldots, z(k-k_s)$, we define the *extended performance*

$$Z(k) \triangleq \left[\begin{array}{c} z(k-k_1) \\ \vdots \\ z(k-k_s) \end{array} \right] \in \mathbb{R}^s. \quad (22)$$

Therefore,

$$Z(k) \triangleq \tilde{\mathcal{S}}(k) + \tilde{\mathcal{H}}\tilde{U}(k-1), \quad (23)$$

where

$$\tilde{\mathcal{S}}(k) \triangleq \left[\begin{array}{c} \mathcal{S}_1(k-k_1) \\ \vdots \\ \mathcal{S}_s(k-k_s) \end{array} \right] \in \mathbb{R}^s,$$

$\tilde{U}(k-1)$ has the form

$$\tilde{U}(k-1) \triangleq \left[\begin{array}{c} \mathcal{P}\big(\mathcal{N}_c(u_{\mathrm{c}}(k-q_1))\big) \\ \vdots \\ \mathcal{P}\big(\mathcal{N}_c(u_{\mathrm{c}}(k-q_{l_{\tilde{U}}}))\big) \end{array} \right] \in \mathbb{R}^{l_{\tilde{U}}},$$

where, for $i = 1, \ldots, l_{\tilde{U}}$, $k_1 \leq q_i \leq k_s + \ell$, and $\tilde{\mathcal{H}} \in \mathbb{R}^{s \times l_{\tilde{U}}}$ is constructed according to the structure of $\tilde{U}(k-1)$. The vector $\tilde{U}(k-1)$ is formed by stacking $U_1(k-k_1-1), \ldots, U_s(k-k_s-1)$ and removing copies of repeated components. Next, for $j = 1, \ldots, s$, we define the *retrospective performance*

$$\hat{z}_j(k-k_j) \triangleq \mathcal{S}_j(k-k_j) + \mathcal{H}_j \hat{U}_j(k-k_j-1), \quad (24)$$

where the past controls $U_j(k-k_j-1)$ in (21) are replaced by the retrospective controls $\hat{U}_j(k-k_j-1)$. In analogy with (22), the *extended retrospective performance* for (24) is defined as

$$\hat{Z}(k) \triangleq \left[\begin{array}{c} \hat{z}_1(k-k_1) \\ \vdots \\ \hat{z}_s(k-k_s) \end{array} \right] \in \mathbb{R}^s$$

and thus is given by

$$\hat{Z}(k) = \tilde{\mathcal{S}}(k) + \tilde{\mathcal{H}}\hat{\tilde{U}}(k-1), \quad (25)$$

where the components of $\hat{\tilde{U}}(k-1) \in \mathbb{R}^{l_{\tilde{U}}}$ are the components of $\hat{U}_1(k-k_1-1), \ldots, \hat{U}_s(k-k_s-1)$ ordered in the same way as the components of $\tilde{U}(k-1)$. Subtracting (23) from (25) yields

$$\hat{Z}(k) = Z(k) - \tilde{\mathcal{H}}\tilde{U}(k-1) + \tilde{\mathcal{H}}\hat{\tilde{U}}(k-1). \quad (26)$$

Finally, we define the *retrospective cost function*

$$J(\hat{\tilde{U}}(k-1), k) \triangleq \hat{Z}^{\mathrm{T}}(k) R(k) \hat{Z}(k), \quad (27)$$

where $R(k) \in \mathbb{R}^{s \times s}$ is a positive-definite performance weighting. The goal is to determine refined controls $\hat{\tilde{U}}(k-1)$ that would have provided better performance than the controls $U(k)$ that were applied to the system. The refined control values $\hat{\tilde{U}}(k-1)$ are subsequently used to update the controller.

Next, to ensure that (27) has a global minimizer, we consider the regularized cost

$$\bar{J}(\hat{\tilde{U}}(k-1), k) \triangleq \hat{Z}^{\mathrm{T}}(k) R(k) \hat{Z}(k) + \eta(k) \hat{\tilde{U}}^{\mathrm{T}}(k-1) \hat{\tilde{U}}(k-1), \quad (28)$$

where $\eta(k) \geq 0$. Substituting (26) into (28) yields

$$\bar{J}(\hat{\tilde{U}}(k-1), k) = \hat{\tilde{U}}(k-1)^{\mathrm{T}} \mathcal{A}(k) \hat{\tilde{U}}(k-1) + \mathcal{B}(k) \hat{\tilde{U}}(k-1) + \mathcal{C}(k),$$

where

$$\mathcal{A}(k) \triangleq \tilde{\mathcal{H}}^{\mathrm{T}} R(k) \tilde{\mathcal{H}} + \eta(k) I_{l_{\tilde{U}}},$$
$$\mathcal{B}(k) \triangleq 2\tilde{\mathcal{H}}^{\mathrm{T}} R(k)[Z(k) - \tilde{\mathcal{H}}\tilde{U}(k-1)],$$
$$\mathcal{C}(k) \triangleq Z^{\mathrm{T}}(k) R(k) Z(k) - 2Z^{\mathrm{T}}(k) R(k) \tilde{\mathcal{H}} \tilde{U}(k-1) + \tilde{U}^{\mathrm{T}}(k-1) \tilde{\mathcal{H}}^{\mathrm{T}} R(k) \tilde{\mathcal{H}} \tilde{U}(k-1).$$

If either $\tilde{\mathcal{H}}$ has full column rank or $\eta(k) > 0$, then $\mathcal{A}(k)$ is positive definite. In this case, $\bar{J}(\hat{\tilde{U}}(k-1), k)$ has the unique global minimizer

$$\hat{\tilde{U}}(k-1) = -\frac{1}{2} \mathcal{A}^{-1}(k) \mathcal{B}(k). \tag{29}$$

The control $u(k)$ is given by the strictly proper time-series controller of order n_{c} given by

$$u(k) = \sum_{i=1}^{n_{\mathrm{c}}} M_i(k) u(k-i) + \sum_{i=1}^{n_{\mathrm{c}}} N_i(k) z(k-i) + \sum_{i=1}^{n_{\mathrm{c}}} Q_i(k) r(k-i), \tag{30}$$

where, for all $i = 1, \ldots, n_{\mathrm{c}}$, $M_i(k) \in \mathbb{R}$, $N_i(k) \in \mathbb{R}$, and $Q_i(k) \in \mathbb{R}$. The control (30) can be expressed as

$$u(k) = \theta(k) \phi(k-1),$$

where

$$\theta(k) \triangleq \left[M_1(k) \; \cdots \; M_{n_{\mathrm{c}}}(k) \; N_1(k) \; \cdots \; N_{n_{\mathrm{c}}}(k) \; Q_1(k) \; \cdots \; Q_{n_{\mathrm{c}}}(k) \right] \in \mathbb{R}^{l_u \times 3n_{\mathrm{c}}}$$

and

$$\phi(k-1) \triangleq \left[u(k-1) \; \cdots \; u(k-n_{\mathrm{c}}) \; z(k-1) \; \cdots \; z(k-n_{\mathrm{c}}) \; r(k-1) \; \cdots \; r(k-n_{\mathrm{c}}) \right]^{\mathrm{T}} \in \mathbb{R}^{3n_{\mathrm{c}}}.$$

Next, let d be a positive integer such that $\tilde{U}(k-1)$ contains $u(k-d)$ and define the cumulative cost function

$$J_{\mathrm{R}}(\theta, k) \triangleq \sum_{i=d+1}^{k} \lambda^{k-i} \| \phi^{\mathrm{T}}(i-d-1) \theta^{\mathrm{T}}(k) - \hat{u}^{\mathrm{T}}(i-d) \|^2 + \lambda^k (\theta(k) - \theta_0) P_0^{-1} (\theta(k) - \theta_0)^{\mathrm{T}}, \tag{31}$$

where $\| \cdot \|$ is the Euclidean norm, and $\lambda \in (0, 1]$ is the forgetting factor. Minimizing (31) yields

$$\theta^{\mathrm{T}}(k) = \theta^{\mathrm{T}}(k-1) + \beta(k) P(k-1) \phi(k-d-1) \cdot [\phi^{\mathrm{T}}(k-d) P(k-1) \phi(k-d-1) + \lambda(k)]^{-1} \cdot [\phi^{\mathrm{T}}(k-d-1) \theta^{\mathrm{T}}(k-1) - \hat{u}^{\mathrm{T}}(k-d)],$$

where $\beta(k)$ is either zero or one. The error covariance is updated by

$$P(k) = \beta(k) \lambda^{-1} P(k-1) + [1 - \beta(k)] P(k-1) - \beta(k) \lambda^{-1} P(k-1) \phi(k-d-1) \cdot [\phi^{\mathrm{T}}(k-d-1) P(k-1) \phi(k-d) + \lambda]^{-1} \cdot \phi^{\mathrm{T}}(k-d-1) P(k-1).$$

We initialize the error covariance matrix as $P(0) = \alpha I_{3n_{\mathrm{c}}}$, where $\alpha > 0$. Note that when $\beta(k) = 0$, $\theta(k) = \theta(k-1)$ and $P(k) = P(k-1)$. Therefore, setting $\beta(k) = 0$ switches off the controller adaptation, and thus freezes the control gains. When $\beta(k) = 1$, the controller is allowed to adapt.

V. Simulation Results

Example 5.1: We consider $G_a(z) = \frac{0.3161}{z-0.3679}$ and $G(z) = 1$, and the generalized Prandtl-Ishlinskii model with $n = 4$, $a_0 = 0.6$, $a_1 = 0.14$, $a_2 = 0.25$, $a_3 = 0.33$, $\rho_0 = 0$, $\rho_1 = 0.223$, $\rho_2 = 0.363$, $\rho_3 = 0.471$. We use $\gamma(u_0) = 1.3 \tanh(u_0)$. We use the command signal $r(k) = 0.8 \sin(\omega k)$ where $\omega = \frac{\pi}{10}$ rad/sample and $\omega = \frac{\pi}{200}$ rad/sample. We let $a = 7$, $n_{\mathrm{c}} = 24$, and $P_0 = 0.12 I_{3n_{\mathrm{c}}}$. The RCAC controller is turned on at $k = 400$. Figure 3 shows the simulation results.

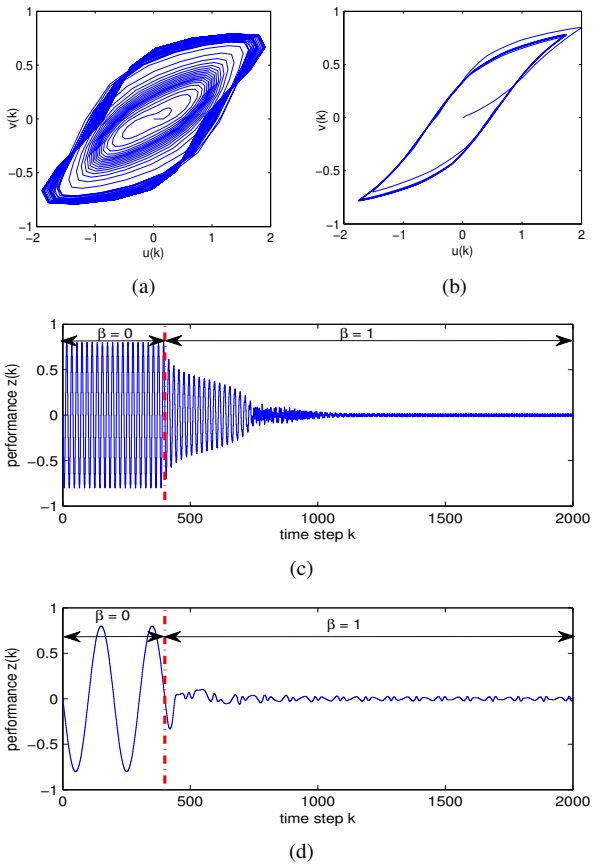

Fig. 3. Example 5.1. (a) and (b) show the output of the SMA model $\mathcal{P}$ with $G_a(z) = \frac{0.3161}{z-0.3679}$, $G(z) = 1$, and the command signal $r(k) = 0.8 \sin(\omega k)$, where (a) $\omega = \frac{\pi}{10}$ rad/sample, and (b) $\omega = \frac{\pi}{100}$ rad/sample. (c) and (d) show the closed-loop response with (a) and (b), respectively.

Example 5.2: In this example we consider the SMA model $\mathcal{P}$ with the oscillatory plant $G(s) = \frac{\omega_{\mathrm{n}}^2}{s^2 + 2\zeta\omega_{\mathrm{n}} + \omega_{\mathrm{n}}^2}$, where ζ is the damping coefficient and ω_{n} is the natural frequency. We consider $G_a(z) = \frac{0.65}{z-0.35}$ and the generalized Prandtl-Ishlinskii Φ model with $n = 4$, $a_0 = 0.6$, $a_1 = 0.4$, $a_2 = 0.2$, $a_3 = 0.1$, $\rho_0 = 0$, $\rho_1 = 0.1$, $\rho_2 = 0.2$, $\rho_3 = 0.4$, and $\gamma(u_0) = \tanh(u_0)$. We use $\omega_{\mathrm{n}} = \frac{\pi}{10}$ rad/sample, $\zeta = 0.4$, and the sinusoidal command $r(k) = 0.8 \sin(\omega k)$

with $\omega = \frac{\pi}{10}$ rad/sample and $\omega = \frac{\pi}{200}$ rad/sample. The disturbance signal is $w(k) = 0.1$. We let $a = 6$, $n_c = 35$, and $P_0 = 0.016 I_{3n_c}$. The RCAC controller is turned on at $k = 400$. Figure 6 shows the simulation results.

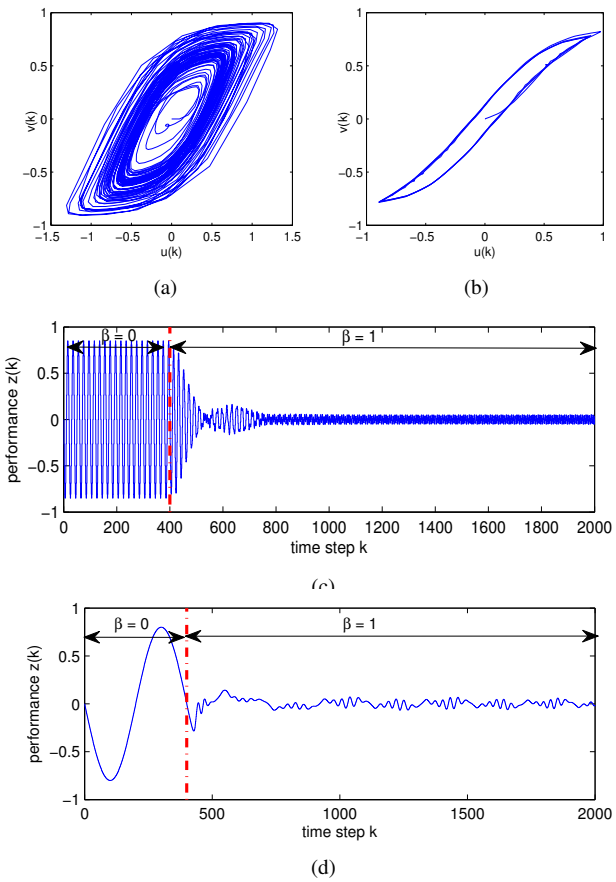

Fig. 4. Example 5.2. (a) and (b) show output of the SMA model $\mathcal{P}$ with $G_a(z) = \frac{0.65}{z-0.35}$, $G(z) = \frac{0.1313z+0.08632}{z^2-1.067z+0.2846}$, and the sinusoidal command $r(k) = 0.8\sin(\omega k)$, where (a) $\omega = \frac{\pi}{10}$ rad/sample, and (b) $\omega = \frac{\pi}{200}$ rad/sample. (c) and (d) show the closed-loop response with (a) and (b), respectively.

VI. Flap Positioning System

We consider the flap positioning system described in [19], where a SMA actuator is used to control the flap position. We use the SMA model $\mathcal{P}$ to characterize the SMA actuator. This system is modeled by

$$J\ddot{y} + \xi\dot{y} + k_s r_d^2 y = k_c \mathcal{P} - w, \tag{32}$$

where $2r_d$ is diameter of the pulley, y is the rotation angle of the pulley, J is the moment of inertia of the pulley and the flap, ξ is the damping coefficient, and $w(k)$ represents the aerodynamic moment applied to the flap.

The parameters are $\sigma = \eta = 1$, $J = 5.0 \times 10^{-5}$ kg-m^2, $\xi = 0.002$ kg-m^2-s^{-1}, $r_d = 2$ cm, $k_s = 8$, and $k_c = 0.1$. Then $G_a(z) = \frac{0.3161}{z-0.3679}$ and $G(z) = \frac{0.5019z+0.00536}{z^2-0.1883z}$. We let $a = 7$, $n_c = 20$, and $P_0 = 0.86 I_{3n_c}$. We consider the command signal $r(k) = 0.8\sin(\omega k)$ with $\omega = \frac{\pi}{10}$ rad/sample, $\omega = \frac{\pi}{20}$ rad/sample, $\omega = \frac{\pi}{50}$ rad/sample, and $\omega = \frac{\pi}{100}$ rad/sample. The disturbance signal is $w(k) = 0.1\sin(\frac{\pi}{20}k)$. The RCAC controller is turned on at $k = 400$. Figure 5 shows the simulation results.

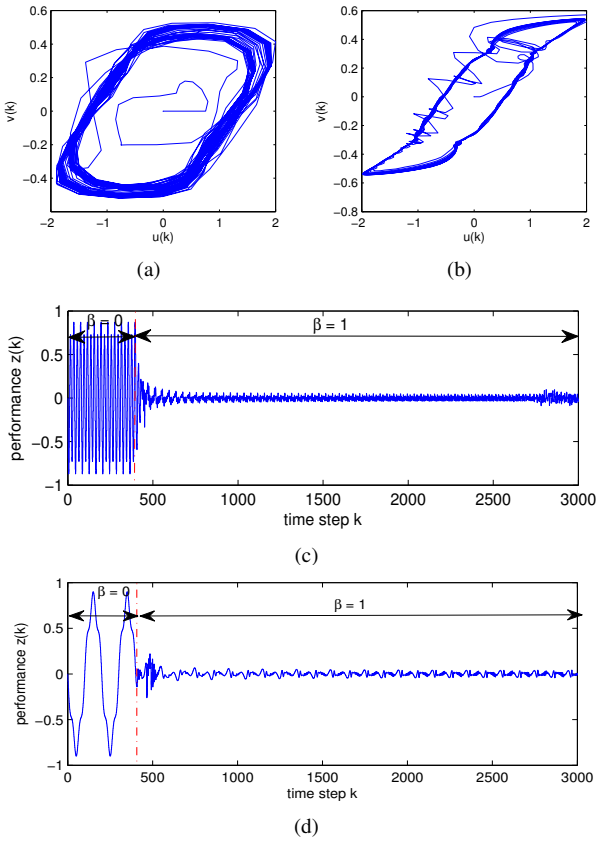

Fig. 5. RCAC with a flap positioning system. (a) and (b) show the position output of the SMA model $\mathcal{P}$ with the command signal $r(k) = 0.8\sin(\omega k)$ and the disturbance signal $w(k) = 0.1\sin(\frac{\pi}{20}k)$ (a) $\omega = \frac{\pi}{10}$ rad/sample and (b) $\omega = \frac{\pi}{100}$ rad/sample. (c) and (d) show the closed-loop response with (a) and (b), respectively.

VII. RCAC with the SMA model and a nonlinear system

We consider a nonlinear system preceded by the SMA model $\mathcal{P}$. Let

$$x(k+1) = \frac{1 - e^{x(k)}}{1 + e^{x(k)}} + \mathcal{P}\big(u(k)\big) + w(k), \tag{33}$$

$$y(k) = x(k). \tag{34}$$

We consider $G_a(z) = \frac{0.5}{z-0.25}$ and the generalized Prandtl-Ishlinskii model with $n = 4$, $a_0 = 0.5$, $a_1 = 0.1$, $a_2 = 0.2$, $a_3 = 0.3$, $\rho_0 = 0$, $\rho_1 = 0.1$, $\rho_2 = 0.2$, $\rho_3 = 0.3$, and $\gamma(u_0) = \tanh(u_0)$. We use the sinusoidal command $r(k) = 2\sin(\omega k)$, where $\omega = \frac{\pi}{20}$ rad/sample and $\omega = \frac{\pi}{200}$ rad/sample. The disturbance signal is $w(k) = 0.1\sin(\frac{\pi}{20}k)$. We let $a = 8$, $n_c = 22$, and $P_0 = 0.01 I_{3n_c}$. The RCAC controller is turned on at $k = 400$. Figure 6 shows the simulation results.

VIII. Conclusions

Retrospective cost adaptive control (RCAC) was applied to a command-following problem involving an uncertain SMA

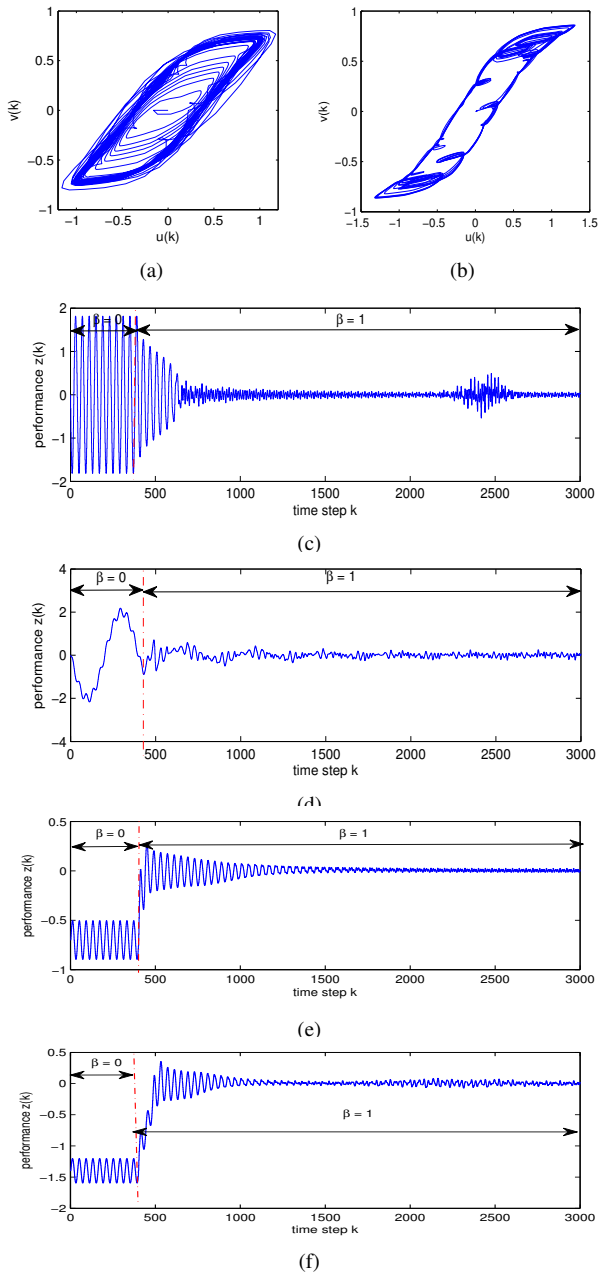

Fig. 6. RCAC with the SMA model and a nonlinear system. (a) and (b) show output of the SMA model $\mathcal{P}$ with $G_a(z) = \frac{0.5}{z-0.25}$, the nonlinear plant $x(k+1) = \frac{1-e^{x(k)}}{1+e^{x(k)}}$, and the sinusoidal command $r(k) = 2\sin(\omega k)$, where (a) $\omega = \frac{\pi}{20}$ rad/sample, and (b) $\omega = \frac{\pi}{200}$ rad/sample. (c) and (d) show the closed-loop response with (a) and (b), respectively. (e) and (f) show the closed-loop response to the constant commands $r(k) = 0.7$ and $r(k) = 1.4$, respectively.

actuator with a linear temperature dynamics model and a hysteresis nonlinearity characterized by a generalized Prandtl-Ishlinskii model. RCAC was used with limited modeling information about the SMA actuator and the plant. RCAC was applied to a flap positioning system actuated by the SMA model. The simulation results show that RCAC can be used to control the SMA actuator followed by an asymptotically stable linear plant without using an inverse hysteresis model in the closed-loop system.

REFERENCES

[1] M. C. Kung and B. F. Womack, "Discrete-time adaptive control of linear dynamic systems with a two-segment piecewise-linear asymmetric nonlinearity," *IEEE Trans. Autom. Contr.*, vol. 29, pp. 170-172, 1984.

[2] G. Tao and P. V. Kokotović, *Adaptive Control of Systems with Actuator and Sensor Nonlinearities*, Wiley, 1996.

[3] J. Yan, A. M. D'Amato, D. Sumer, J. B. Hoagg, and D. S. Bernstein, "Adaptive Control of Uncertain Hammerstein Systems Using Auxiliary Nonlinearities," *Proc. Conf. Dec. Contr.*, Maui, HI, 2012, pp. 4811-4816.

[4] M. Al Janaideh, J. Yan, A. M. D'Amato, and D. S. Bernstein, "Retrospective-Cost Adaptive Control of Uncertain Hammerstein-Wiener Systems with Memoryless and Hysteretic Nonlinearities," *AIAA Guid. Nav. Contr. Conf.*, Minneapolis, MN, August 2012, AIAA-2012-4449-671.

[5] R. Venugopal and D. S. Bernstein, "Adaptive Disturbance Rejection Using ARMARKOV System Representations," *IEEE Trans. Contr. Sys. Tech.*, vol. 8, pp. 257-269, 2000.

[6] J. B. Hoagg, M. A. Santillo and D. S. Bernstein, "Discrete-Time Adaptive Command Following and Disturbance Rejection for Minimum-Phase Systems with Unknown Exogenous Dynamics," *IEEE Trans. Autom. Contr.*, vol. 53, pp. 912-928, 2008.

[7] J. B. Hoagg and D. S. Bernstein, "Retrospective Cost Adaptive Control for Nonminimum-Phase Discrete-Time Systems Part 1: The Ideal Controller and Error System; Part 2: The Adaptive Controller and Stability Analysis," *Proc. Conf. Dec. Contr.*, pp. 893-904, Atlanta, GA, December 2010.

[8] M. Aljanaideh, D. Sumer, J. Yan, A. M. D'Amato, B. Drincic, K. Aljanaideh, and D. S. Bernstein, "Adaptive Control of Uncertain Hammerstein Systems with Uncertain Hysteretic Input Nonlinearities," *Proc. Dyn. Sys. and Contr. Conf.* , Fort Lauderdale, FL, October 2012, DSCC2012-MOVIC2012-8573, pp. 1-10.

[9] A. M. D'Amato, E. D. Sumer, and D. S. Bernstein, "Retrospective Cost Adaptive Control for Systems with Unknown Nonminimum-Phase Zeros," *AIAA Guid. Nav. Contr. Conf.*, Portland, OR, August 2011, AIAA-2011-6203.

[10] M. S. Fledderjohn, M. S. Holzel, H. Palanthandalam-Madapusi, R. J. Fuentes, and D. S. Bernstein, "A Comparison of Least Squares Algorithms for Estimating Markov Parameters," *Proc. Amer. Contr. Conf.*, Baltimore, MD, June 2010, pp. 3735-3740.

[11] J. A. Shaw, "Simulations of localized thermo-mechanical behavior in a NiTi shape memory alloy," *Inter. J. Plast.*, vol. 16, pp. 541-562, 2000.

[12] R. Gorbet, K. Morris and D. Wang, "Passivity-Based Stability and Control of Hysteresis in Smart Actuators," *IEEE Trans. Contr. Sys. Tech.*, vol. 9, pp. 5-16, 2001.

[13] M. Elahinia and H. Ashrafiuon, "Nonlinear Control of a Shape Memory Alloy Actuated Manipulator," *J. Vib. Acous.*, vol. 124, pp. 566-575, 2002.

[14] Y. Feng, C. Rabbath, H. Hong, M. Al Janaideh, and C-Y. Su, "Robust Control for Shape Memory Alloy Micro-Actuators Based Flap Positioning System," *Proc. Amer. Contr. Conf.*, Baltimore, MD, June 2010, pp. 4181-4186.

[15] M. Al Janaideh, S. Rakheja, and C-Y. Su, "An Analytical Generalized Prandtl-Ishlinskii Model Inversion for Hysteresis Compensation in Micro positioning Control," *IEEE/ASME Trans. Mech.*, vol. 16, pp. 734-744, 2011.

[16] M. Al Janaideh, S. Rakheja, and C-Y. Su, "A Generalized Prandtl-Ishlinskii Model for Characterizing Hysteresis Nonlinearities of Smart Actuators," *Smart Mater. and Struct.*, vol. 18, pp. 1-9, 2009.

[17] M. Al Janaideh, Y. Feng, S. Rakheja, Y. Tan, and C-Y. Su, "Generalized Prandtl-Ishlinskii Hysteresis: Modeling and Robust Control," *Proc. Conf. Dec. Contr.*, Shanghai, China, December 2009, pp. 7279-7284.

[18] M. Al Janaideh, Y. Feng, S. Rakheja, C-Y. Su, C. Rabbath, "Hysteresis compensation for smart actuators using inverse generalized Prandtl-Ishlinskii model," *Proc. Amer. Contr. Conf.*, St. Louis, MO, June 2009, pp. 307-312.

[19] N. Lechevin, C.A. Rabbath, F. Wong, and O. Boissonneault, "Synthesis and Experimental Validation of Two-Step Variable- Structure Control of a Micro-Actuated Flow Effector," *Proc. Amer. Contr. Conf.*, New York, NY, July 2007, pp. 3210- 3215.